

ORIGINAL CONTRIBUTION

Utilizing Superpave Gradations to Assess Permanent Deformation and Fracture in HMA Mixes

Muhammad Haris Javed^{1*}, Inam Ur Rehman², Murad Khan³, Akhtar Abbas⁴, Adnan Khan⁵¹ Missouri University of Science and Technology, Rolla, MO² Hefei University of Technology, Hefei, Anhui, China³ Tianjin University, Tianjin, China⁴ Pakistan Institute of Engineering and Technology (PIET), Multan, Pakistan⁵ CECOS University of IT and Emerging Sciences, Peshawar, Pakistan

Abstract— This research study investigates the Fatigue Failure & Permanent Deformation response behaviour of four (04) HMA mixtures. The selected gradations have a Nominal Maximum Aggregate Size (NMAS) of 19.0 mm, and the gradation blends passed Above (ARZ), Below (BRZ), and Through (TRZ), the restricted zone. Along with the Superpave ARZ, BRZ & TRZ conventional NHA, “Class A” gradation was also checked for performance parameters, thus producing results in contrast to the conventional NHA gradation already used by highway industries Pakistan. Three (03) performance tests were carried out in this study that, includes Indirect Tensile Strength Test (IDT), the repeated Indirect Tensile Fatigue Test (ITFT), and the Moisture Susceptibility Test. Statistical analysis was also done based on laboratory-produced results. Two-Level Factorial Design was also carried out using the statistical tool Minitab-16. Statistical analysis shows that OBC, $P_{0.075}/P_{be}$ (Dust to Binder Ratio), and the Peak Force significantly affect No of Cycles to Fatigue Failure. A linear Model was developed with an R square of .74 which seems to fit well. IDT Test evaluated the TRZ mix as having the best laboratory fracture resistance properties of all tested mixes, while ARZ performed best in the Moisture Susceptibility test. Moreover, this study gave us insight into Superpave IDT as a practical and reliable way to measure all the parameters needed in the HMA Fracture Mechanics method.

Index Terms— Tensile Strength, Fatigue Failure, Permanent Deformation, Superpave Gradations

Received: 10 February 2022; Accepted: 03 April 2022; Published: 20 June 2022



© 2022 JITDETS. All rights reserved.

I. INTRODUCTION

Transportation plays a significant part in the daily life of human beings. The better the transportation system and infrastructure, the more developed the country is [1]. Transportation infrastructure is the keystone to the development of any country. Pakistan is among the developing countries where roads are the major contributor to the transportation infrastructure responsible for the movement of people and goods [2]. The entire roadway network in Pakistan is approximately 264,415 km comprising 9324 km of National Highways and 2280 km of Motorways that serve millions of people, commuters, automobiles, trucks, etc., daily. The preservation of this huge infrastructure needs suitable and cost-effective design, maintenance, and rehabilitation practices [3, 4]. Adopting an appropriate design road will decrease the maintenance cost and provide a safe and comfortable ride to commercial and private vehicles. Such pavements will have a long life, increasing the country's socioeconomic growth. Asphalt pavements are very common these days around the world. Much emphasis is being done on making asphalt pavements that are long-lasting and can provide the desired level of comfort and ease, thus serving the purpose

for which they are intended [5]. The economic and satisfactory design also significantly affects Hot Mix Asphalt (HMA) pavement structures like other engineering structures. In Pakistan, a significant portion of road infrastructure consists of asphalt concrete (AC), and pavement distress associated with pavement structure includes fatigue cracking, stripping, rutting, ageing and travelling, etc. [6, 7, 8]. Due to these distresses, the pavement fails before completing its service life and needs maintenance and rehabilitation, which in turn causes a massive burden on the nation's economy. Cracking is among the most significant distress modes in flexible or asphalt pavements. Cracks initiate and then propagate in the asphalt pavements due to combined impact from both environmental variations and traffic loading [9].

To a great extent, crack initiation governs the service life of the asphalt structure; once the crack has initiated, it will act as a stress concentration and facilitate the entrance of moisture into the pavements. The major performance problem associated with HMA is fatigue cracking. Fatigue, as considered in this research study, is a form of cracking resulting from repeated traffic loading or load application [10]. In contrast to fatigue, another term is also used: fracture. A fracture occurs as a result of fatigue,

* Corresponding author: Muhammad Haris Javed

† Email: harisjaved055@gmail.com

and many other distresses. Therefore, for clarification, it is noteworthy that throughout this thesis, “fatigue resistance” denotes the ability of HMA mixes to resist cracking due to repeated loading.

Consequently, fatigue cracking will lead to accelerated pavement deterioration, thus leading to premature failure and high maintenance costs. Characterizing the fatigue resistance properties of asphalt mixture is critical for improving the performance-related mixture design [11]. Characterizing fatigue resistance of asphalt mixtures is not a straightforward task as the mechanical properties of HMA depend on the mode of loading, temperature, and time. However, a fundamental energy-based threshold governs the fracture initiation in asphalt – the dissipated creep strain energy threshold. Super pave is extensively used and overcomes earlier methods’ deficiencies and insufficiencies. There was a necessity to characterize the mechanical properties of HMA, and for this purpose, National Cooperative Highway Research Program (NCHRP) brought about several studies [12]. As a result, they concluded that fatigue cracking as a distressed type can best characterize the mix produced using the super pave gyratory compactor. It can also complement the super pave volumetric design too. This method is comparatively new for Pakistan and is still to be entirely implemented. Before implementing this technique, it is vital to perform laboratory assessments of different bitumen mixes, thus predicting their response in the field along with the co-relation of laboratory results with the field results. The comparison and co-relation can be best made among the super pave gradations in contrast to the Gradation already used in the field or industry, i.e., NHA Gradation. In this regard, fatigue cracking in terms of the IDT, Repeated Indirect Tensile Fatigue Test (as a surrogate of the Number of Load Cycles to Fatigue Failure), and Moisture Susceptibility are the lead candidates as performance tests.

Fatigue cracking of asphalt pavement depends on the horizontal tensile strain emerging at the bottom of the bituminous layer due to repeated traffic loading [13, 14, 15, 16]. Starting as micro cracks, these cracks disseminate, densify, and amalgamate to form macro cracks, a development directly related to stress-strain fields in asphalt layers. Accurate prediction of fatigue behaviour requires an in-depth understanding of the characteristics of HMA under realistic traffic conditions [13]. Aggregate and binder are two major HMA components. By changing aggregate source, the properties of HMA also vary.

Similarly, a change in binder grade will vary the properties of HMA. This chapter comprehensively reviews the literature regarding Superpave Mix design, its properties, and, most importantly, the restricted zone concept. The theory about the UTM-25 used for the Repeated Indirect Tensile Fatigue Test, the IDT, and the Moisture Susceptibility is also explained in detail. Factors affecting them, the Statistical Software’s usage, and the Experiment’s Design are also described.

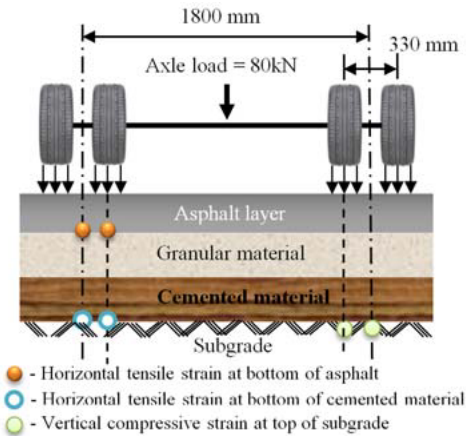


Fig. 1. Types of Strains in Pavement

Super pave defines guidelines for aggregate selection procedures after procurement of aggregate from native sources. This procedure includes consensus properties and source properties of aggregates.

Consensus properties include Fine Aggregate Angularity (FAA), Coarse Aggregate Angularity (CAA), flat & elongated particles, and clay content. FAA and CAA mean that “aggregate particles must be angular/rough so that they can provide adequate internal friction to resist permanent deformation and shear resistance”, whereas “flat and elongated particles should be avoided because they cause problems in handling and break during construction or traffic loading”. To form the durable mix that forms adhesion between aggregate and binder by limiting clay content.

TABLE I
SUPERPAVE AGGREGATE CONSENSUS PROPERTY REQUIREMENT

| Design ESALs (Millions) | Coarse Aggregate Angularity (Percent), Minimum | | Un Compacted Void Content of Fine Aggregate (Percent), Minimum | | Sand Equivalent (Percent), Minimum | Flat and Elongated (Percent), Maximum |
|-------------------------|--|----------|--|----------|------------------------------------|---------------------------------------|
| | ≤ 100 mm | > 100 mm | ≤ 100 mm | > 100 mm | | |
| | < 0.3 | 55/- | -/- | - | | |
| 0.3 to < 3 | 75/- | 50/- | 40 | 40 | 40 | 10 |
| 3 to < 10 | 85/80 | 60/- | 45 | 40 | 45 | 10 |
| 10 < 30 | 95/90 | 80/75 | 45 | 40 | 45 | 10 |
| ≥ 30 | 100/100 | 100/100 | 45 | 45 | 50 | 10 |

Source properties include soundness, toughness, and deleterious test. A soundness test is conducted to find the environmental effect on aggregates like the freeze and thaw effect. The toughness test ensures that particles are strong enough to bear wear and tear, and the deleterious test that helps is a selection of material with no less percentage of contaminants like wood, mica, clay lumps, shale, and coal.

Superpave modifies the gradation approach by introducing a 0.45 power gradation chart that defines permissible Gradation [17]. The chart’s Ordinate (vertical axis) expresses the percentage passing whereas the abscissa (horizontal axis) size in millimetres to power 0.45. The Maximum

Density Line (MDL) represents a gradation where the particle size is fixed in the densest possible agreement [18, 19]. The stability of asphalt concrete pavement is largely dependent upon aggregate properties. Gradation is a very important property of aggregate that determines mix stability. Mixes having different gradations have different stiffness and cracking potential. The Gradation above the restricted zone is termed a delicate mix, whereas the Gradation passing below the restricted zone is termed a rough mix [17]. Control point position in Superpave Gradation varies depending on NMAS. Boundaries of the restricted zone are also dependent upon NMAS.

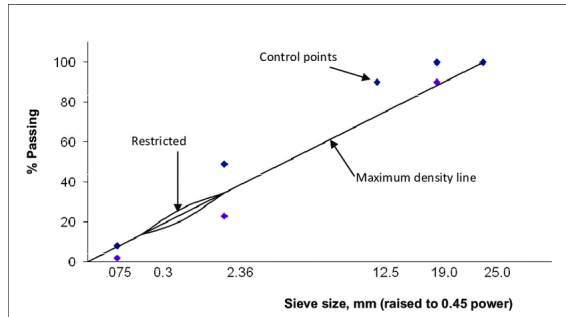


Fig. 2. Super Pave Gradation Limit

In Super pave, the restricted zone is a zone that is disregarded, and it was proposed that the Gradation passing through the restricted zone will produce a tender mix, cause difficulty in compaction, and would not produce durable mixes. The restricted zone was introduced to minimize the effect of poor volumetric properties, fine and rounded sand, and develop a solid aggregate structure [20]. The restricted zone concept was adopted to avoid premature failure. It was also proposed that Gradation passing through the RZ will produce mixes that will be susceptible to damage, but the researchers concluded that the performance of the mixes passing through and above the RZ would perform better than mixes below or above the restricted zone. The effect of Gradation on the resistance of HMA mixtures to permanent deformation was evaluated.

For this reason, five different Superpave gradations (two passing through, two passing below, and one above the restricted zone) in compliance with the restricted zone were considered. A usual trend observed was that coarser gradation mixtures below the restricted zone are more prone to fatigue damage than fine-graded mixtures. The HMA Fracture Mechanics has been extensively evaluated. It is seen that IDT allows us to successfully distinguish between the Superpave mixtures with good and bad fracture resistance. Superpave Gyrotory Compactor (SGC) was introduced to comply with the laboratory-fabricated sample by SHRP and is considered a key feature of the Superpave mix design procedure [21]. The main goal of the SGC is to produce a specimen that represents the in-field performance of the pavement. The samples are compacted per the traffic volume expected on roads and climatic conditions. The laboratory-fabricated sample densities were continuously measured during compaction. SGC has a reaction frame, loading ram, height measurement, and mold and control data acquisition panel. Implementing the M-EPDG requires comprehensive characterization and evaluation of lab-produced mixtures and field results. The purpose of this research study is as follows:

- To investigate the Wearing Course Super pave Gradation blend (ARZ, BRZ, and TRZ) that performs better against fatigue cracking using UTM -25.
- To investigate the Wearing Course NHA "Class A" blend that performs better against fatigue cracking and compare it with the already calculated results of Super pave Gradations.
- To estimate a trend of load cycles (Repeated Indirect Tensile Fatigue Test) to create a permanent deformation in samples and thus compare results among different gradations.
- To investigate the factors that affect the ITFT (fatigue parameter) to compare the different asphalt concrete mixes (Superpave & NHA

"A" Gradations).

- To check for significant factors among the Superpave Volumetric that affect the No of Cycles to Fatigue Failure.
- To investigate the aggregate gradation blend that is more moisture susceptible.

II. MATERIALS AND METHOD

Based on the optimum asphalt content calculated using the Marshall Mix technique, the samples were made using SGC. The performance testing, i.e., IDT, Repeated Indirect Fatigue Tests (ITFT) & Moisture Susceptibility tests, were performed on the specimens prepared for the said mixes. The subsequent headings also discuss the additional explanation of the gradations, compaction procedures, and conditioning of samples. The methodology shows that mix Gradation was selected initially, while Optimum Bitumen Content (OBC) was later calculated using the Marshall procedure. This Marshall method determines volumetric properties, including flow and stability, which provides the foundation for testing like fatigue cracking. The calculated OBC is then used to prepare the specimens compacted by a gyrotory compactor which were further cored cut and sawed cut to the requisite size for testing. The indirect tensile test, repeated indirect tension test, and moisture susceptibility test is performed on the gyrotory specimens, and the result is extracted from the software input for the statistical analyses in statistical software PASW 18 and Minitab-16.

Firstly the aggregate is procured from Margalla quarry, whereas the 60/70 grade binder is procured from Attock Oil Refinery. Aggregates are characterized according to standard specifications. Similarly, bitumen is also characterized accordingly to the given set of specifications. Both the aggregate and the binder meet the standard specification requirements. The aggregate and binder mixture is prepared, and the optimum binder content of the gyrotory compacted specimen is determined according to standard specifications for the job mix formula in SP-2.

After the calculation of the OBC, the specimens are made accordingly. Three performance tests were performed according to the standards: indirect tensile strength, indirect tensile fatigue, and moisture susceptibility. Subsequently, an analysis of the result achieved from the performance test is done. This analysis part includes both the performance modelling and the two-level factorial designs. Significant factors were seen that effects the No of cycles to fatigue failure. Based on the test results and the statistical analysis portion, conclusions and recommendations were made accordingly. Conclusions included both the conclusions related to the equipment and testing and the conclusions related to the different types of mixes performed under different tests. The flow chart below displays the methodology step-wise in detail deployed in this research study. Asphaltic concrete is composed of aggregate and bitumen. Margalla crush and Attock Oil Refinery 60/70 penetration grade bitumen is widely used for the construction of pavement in Pakistan and is also used for this research.

A. Aggregate Characterization

Super pave specification divides the aggregates into two properties one is consensus property, and the other one is source property. Consensus properties are critical for the good performance of asphalt mixtures, whereas source property is related to the asphalt mixture performance.

TABLE II
AGGREGATE CHARACTERIZATION

| Test Type | Designation | 1+ / 2+ Fractured Particle | % Air Voids | % Flat/Elongated | % Sand Equivalent% | % Criteria |
|---------------------------------|-------------|----------------------------|-------------|------------------|--------------------|-------------|
| Coarse Aggregate Angularity | ASTM D5821 | 96/92 | - | - | - | 95/90 (min) |
| Fine Aggregates Angularity | ASTM C1252 | - | 50 | - | - | 45 (min) |
| Flat, Elongated Particle | ASTM D4791 | 0 | - | 0 | - | 10 (max) |
| Clay Content (Sand Equivalency) | ASTM D2419 | 48 | - | - | 48 | 45(min) |

60/70 penetration grade bitumen laboratory testing is carried out, and the results are presented in table.

TABLE III
LABORATORY TEST PERFORMED ON ASPHALT

| Test Type | Designation | Test Results |
|---------------------|-------------|--------------|
| Penetration @ 25 °C | ASTM D5 | 63 |
| Flash Point | ASTM D92 | 229 ° C |
| Specific Gravity | ASTM D70 | 1.043 |
| Ductility | ASTM D113 | 104 |

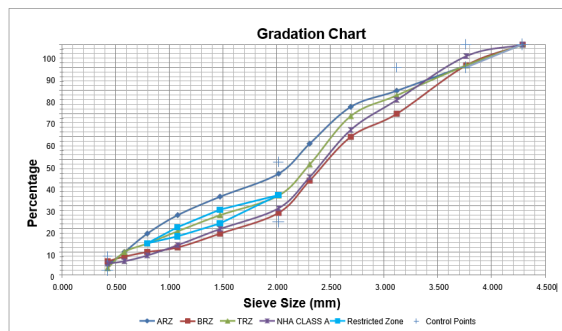


Fig. 3. Gradation Chart

B. Mix Design

Mix design was performed on the entire aggregate structure blend. The Superpave method is followed for mixed design. The respective quantity of each sieve size is placed in a separate bin to achieve the required aggregate blend for each Gradation (ARZ, TRZ, BRZ, and NHA Class A). Sieve material is removed from respective buckets to achieve the required gradation blend. The measured material is placed in a flat tray using balance to estimate the exact quantity. Initially, a trial blend is prepared for each aggregate Gradation. Trial blends were prepared by varying 0.5% bitumen content. The trial blend is due to the mix selection that performs optimally at minimum bitumen content at 4% air voids. Steel trays were first cleansed with petrol before placing the crush into the tray, and the tray was covered with a paper sheet. The weight of each sieve material is batched out from the respective bins and placed into a tray using a scoop. Three trial samples for each Gradation are prepared by varying amounts of bitumen, each weighing approximately 7200g.

1) Heating of material and material mixing

The tray was placed in the oven when the 7200 g material was placed in the tray. For about one and a half hours material is placed in the oven to achieve an appropriate uniform mixing temperature. A temperature gun was used to observe the aggregate temperature until the aggregate achieved 170 °C temperatures.

The mechanical equipment was turned on, and the hand started mixing the material. The temperature was continuously checked with the help of a temperature gun. The mixing process will continue until bitumen coats

the aggregate completely and a uniform mix is obtained. The material is removed from the bucket when the binder completely coats the aggregate. The mixed material was removed from the mechanical bucket and placed in a tray for short-term ageing. The mixed material is kept in an oven for one and a half hours at 135 °C, and mix material is stirred after 30 minutes for a homogenous ageing process; otherwise outer material is more aged than the inner material because of exposure. The short-term ageing process represents the mixing and placement of bituminous mix and allows bitumen to penetrate aggregate pores. When the material was placed into an oven for ageing, the SGC mold was also placed into the oven. The SGC mold was removed from the oven and oiled from all sides. The top plate of mold is taken, and filter paper is cut according to plate size. The filter papers were placed at the bottom and the top of the bituminous mix. After one and a half hours, the material was removed from the oven and poured into an SGC mold. The material was placed in SGC mold with the help of a scoop care should be taken so that no material should be lost while placing the material from the tray into the mold.

2) Gyrotory compacted specimen and volumetric

The sample was compacted according to the Superpave design method up to the desired gyration number using a SGC. The number of gyrations depends upon the expected traffic level on the roads. SGC is attached to the computer. The first mold was placed in SGC and locked with the help of a handle. All the desired variables, like the number of gyrations, angle, and speed, were adjusted in SGC software. The compressor was turned on when all the variables were set, and the mold was locked in the compactor. Start the compacting button, and SGC compacts the specimen at the desired number of gyrations. After compaction, the specimen up to the required number of gyrations was removed from the mold with help of hydraulic remover equipment. The material was not removed immediately from the mold. Steel plate and filter paper are removed from the top of the specimen.

3) Cutting of asphalt mixtures specimen

All the specimens prepared through the SGC have a diameter of 150 mm and a height of 160 mm. As per standard specification for testing in UTM, the specimens were core cut having a 100 mm diameter and 40 mm height for all IDT, ITFT & Moisture Susceptibility Tests. Specimens heights are checked after saw cutting.

C. Indirect Tensile Strength

According to ASTM 6931, standard indirect tensile strength at 25 °C of the compacted gyrotory specimen was conducted to determine tensile strength. The Specimen is placed in temperature controlled cabinet. Actuator is moved up, and the specimen is placed in the jig. To hold the specimen loading strip is placed over the top of the core cut specimen. Actuator is moved down and makes contact with the loading strip. The stress-strain template was opened, and the stress-strain test was conducted by applying a compressive load of 50 mm/min at 25 °C.

III. RESULTS AND DISCUSSIONS

Following are the results of the different performances

A. Test Results and Analysis of Gradations

Mix design results of 19.0 mm NMAS having four (04) different aggregate structures, including volumetric properties. Super pave volumetric properties encompass Air Voids, VFA, %Gmm @ Nini., %Gmm @ Nmax, Design Pb, and Design Pbe. Samples were compacted at 4% air voids. Optimum Asphalt Content was also calculated on 4% Air Voids and volumetrics were investigated (Table IV). VFA is a function of air voids and VMA, and none of the mixes failed at %Gmm @ Nmax; that was why neither value was involved. Based on the linear model developed, VFA, Peak Force, and Dust to Binder Ratio were significant, producing a model with an R Square value of 0.719.

TABLE IV
VOLUMETRIC OF SUPER PAVE GRADATIONS

| Graduation | %VFA | %Gmm @ N_{ini} | Design P_b % | Design P_{be} % | $P_{0.075}/P_{be}$ |
|------------|-------|------------------|----------------|-------------------|--------------------|
| ARZ | 71.00 | 87.90 | 4.30 | 3.82 | 1.17 |
| BRZ | 70.10 | 84.20 | 4.20 | 4.10 | 1.46 |
| TRZ | 69.70 | 85.60 | 4.00 | 3.97 | 1.13 |
| NHA A | 65.08 | 87.76 | 4.10 | 4.05 | 1.23 |

B. Repealed indirect tensile fatigue test

As presented earlier, the ITFT was conducted at 25°C. Volumetric properties show that ARZ has a higher VFA than BRZ, TRZ, and NHA A. Two other factors were considered, including the Dust to Binder Ratio and the Peak Force for the development of the model. Each set of the given equation was checked against the given parameters. The curve estimation technique was used for this purpose. The Goodness of Fit (R square) value was compared, and the significance of variables was also given due consideration. Out of eight (08) variables, only three (03) variables were significant. Linear modelling was done.

TABLE V
ITFT TEST RESULTS FOR GRADATIONS

| Peak Force | Graduation | | | |
|------------|------------|------|------|-------|
| | ARZ | BRZ | TRZ | NHA A |
| 2000 N | 1811 | 461 | 1142 | 1611 |
| 2500 N | 1536 | 354 | 975 | 1311 |
| 3000 N | 1316 | 2283 | 809 | 1061 |
| 3500 N | 1061 | 180 | 626 | 786 |
| 4000 N | 751 | 130 | 441 | 551 |
| 4500 N | 532 | 75 | 241 | 301 |
| 5000 N | 266 | 33 | 154 | 141 |
| 5500 N | 116 | 4 | 26 | 16 |

The figure shows the outcome of Gradation on No of Cycles to Fatigue Failure. TRZ has a marginally higher No of Cycles to Fatigue Failure than BRZ. NHA A is the best performing among all four (04) gradations, even better than the Superpave gradations too. ARZ shows a higher Number of Cycles to Fatigue Failure at higher peak forces, but NHA A performs the best at a low force value. Overall a good trend is seen among the gradations with very clear results, thus making a good analysis. The Goodness of Fit for all of these curves comes out to be around 95%, validating the results as the best fit for a given model.

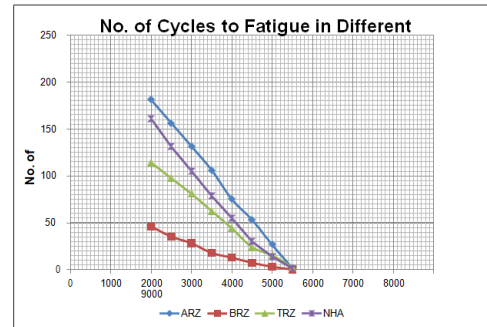


Fig. 4. Effect of Gradation on No of Cycles to Failure/Cycles

Analysis of factors for the model building was evaluated by conducting ANOVA. The table represents the Descriptive Variables from which the model is built. This model is built on the test results conducted on the ITFT test results. Linear Regression was done, and the results were compiled based on the test result analysis.

TABLE VI
DESCRIPTIVE STATISTICS

| | Mean | Std. Deviation | N |
|--------|-----------|----------------|----|
| Cycles | 650.5000 | 614.42372 | 64 |
| Force | 3750.0000 | 1154.70054 | 64 |
| Obc | 4.1500 | .11269 | 64 |
| Dust | 1.2600 | .11989 | 64 |

TABLE VII
CORRELATIONS OF VARIABLES

| | Cycles | VFA | Dust | Force |
|---------------------|--------|-------|-------|-------|
| Pearson Correlation | CYCLES | 1.000 | -.749 | -.068 |
| | FORCE | -.749 | 1.000 | .000 |
| | OBC | .068 | .000 | 1.000 |
| | DUST | -.368 | .000 | .357 |
| Sig. (1-tailed) | CYCLES | . | .000 | .296 |
| | FORCE | .000 | . | .500 |
| | OBC | .296 | .500 | . |
| | DUST | .001 | .500 | .002 |
| N | CYCLES | 64 | 64 | 64 |
| | FORCE | 64 | 64 | 64 |
| | OBC | 64 | 64 | 64 |
| | DUST | 64 | 64 | 64 |

For the sake of software and simplicity, only Labels were given in the software. Here the Cycles represent "No of Cycles to Failure", the Response/Y Variable/Dependent Variable. While the Force is the "Peak Force", Dust refers to the "Dust to Binder Ratio, i.e., $P_{0.075}/P_{be}$ ", and VFA are the "Voids Filled with Asphalt" are the X Variables/Independent Variables.

TABLE VIII
VARIABLES ENTERED/REMOVED IN THE MODEL^B

| Model | Variables Entered | Variables Removed | Method |
|-------|-------------------------------|-------------------|--------|
| 1 | FORCE, DUST, OBC ^a | - | Enter |

Performance testing is the extent of pavement performance when exposed to weather changes or environments, loading patterns or forces, temperature Etc. The mechanistic portion of the recently augmented AASHTO 2002 M-EPDG design guide is built on the development of models to calculate pavement performance and distresses like fatigue cracking,

moisture susceptibility Etc. that deteriorate its service life. Therefore it is imperious to expect pavement performance at the design stage for the permanency and durability of pavement. In such case, No of Cycles to Fatigue Failure/Cycles seems to be a good performance indicator, and its dependence on the Peak Force (Force), $P_{0.075}/P_{be}$ (Dust Proportion/ Dust to Binder Ratio of the Gradation), and OBC also exhibit their role in depicting the performance of the pavement. The data attained from laboratory testing was used to build a model to predict the No of Cycles to Fatigue Failure.

Primarily hit & trail technique was implemented, and scatter plots were produced (using the curve estimation technique) to conform to the best relation of No of Cycles to Fatigue Failure to its affecting variables. By iterative process, several functional forms like linear, exponential, and logarithmic were checked, and many of them emerged as good, but their goodness of fit (R Square) was becoming less. So it is seen that a problem arises when model validation is done because it predicts the response. For the sake of simplicity and ease, the Linear functional form is nominated. This functional form is extensively used to demonstrate the interaction of two or more inputs having a linear relationship and is also used in cost-based empirical studies in many research studies. This functional form is

also prevalent in many engineering economics concepts because it effectively captures the variation. The parameters/ coefficients of independent variables are presented in Equation 1. The general generic functional form was built by using linear regression. The equation for the model is:

$$\text{Cycles} = -127.607 - 0.398 \text{ Force} + 1247.233\text{OBC} - 2304.891P_{0.075}/P_{be} \quad (1)$$

Where,

Cycles = No of Cycles to Fatigue Failure,

Force = Peak Force,

$P_{0.075}/P_{be}$ = Dust Proportion/Dust to Binder Ratio of the Gradation,

and

OBC = Optimum Bitumen Content

The table shows the model parameters and their statistics. It can be concluded that the model is capturing 74 percent of the variation in Cycles/No of Cycles to Failure (Y/response variable) while all the independent variables are significant as their t-stat is greater than the critical value of t-stat at 95% confidence level, i.e., 2.308.

TABLE IX
MODEL SUMMARY^B

| Model | R | R Square | Adjusted R Square | Std. The error in the Estimate | Durbin-Watson |
|-------|-------------------|----------|-------------------|--------------------------------|---------------|
| 1 | .861 ^a | .742 | .729 | 320.09516 | .769 |

a. Predictors: (Constant), FORCE, DUST, OBC

b. Dependent Variable: CYCLES

TABLE X
ANOVA^B

| Model | Sum of Squares | df | Mean Square | F | Sig. |
|------------|----------------|----|-------------|--------|-------------------|
| Regression | 17640200.403 | 3 | 5878628.448 | 57.374 | .000 ^a |
| 1 Residual | 6147654.657 | 60 | 102460.911 | | |
| Total | 23783540.000 | 63 | | | |

a. Predictors: (Constant), FORCE, DUST, OBC

b. Dependent Variable: CYCLES

TABLE XI
COEFFICIENTS^A

| Model | Unstandardized Coefficients | | Standardized Coefficients Beta | t | Sig. | Collinearity Statistics | |
|------------|-----------------------------|------------|-----------------------------------|---------|------|-------------------------|-------|
| | B | Std. Error | | | | Tolerance | VIF |
| (Constant) | -127.607 | 1495.853 | | -.085 | .932 | | |
| FORCE | -.398 | .035 | -.749 | -11.405 | .000 | 1.000 | 1.000 |
| OBC | 1247.233 | 383.148 | .229 | 3.255 | .002 | .872 | 1.146 |
| DUST | -2304.891 | 360.117 | -.450 | -6.400 | .000 | .872 | 1.146 |

a. Dependent Variable: CYCLES

TABLE XII
RESIDUALS STATISTICS^A

| | Minimum | Maximum | Mean | Std. Deviation | N |
|----------------------|------------|-----------|----------|----------------|----|
| Predicted Value | -445.1998 | 1672.9618 | 650.5000 | 529.08854 | 64 |
| Residual | -712.03632 | 956.63159 | .00000 | 312.38089 | 64 |
| Std. Predicted Value | -2.071 | 1.932 | .000 | 1.000 | 64 |
| 2Std. Residual | -2.224 | 2.989 | .000 | .976 | 64 |

a. Dependent Variable: CYCLES

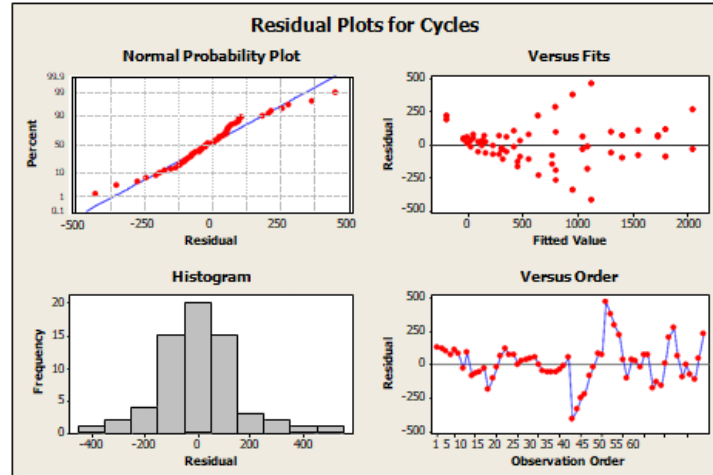


Fig. 5. Residual Plot for Cycles (Y/Response Variable)

C. Design of Experiment

The experiment design is “the grouping of several variables nominated for a research study to recognize the influence of these variables to response”. It is quite a convenient method because, as an alternative to studying the effect of a single factor on the response variable separately, this can help to study the effect of all variables as a combined effect on the response variable. Moreover, testing should not be done for every distinct variable as it makes it more challenging to study when the total numbers of factors are far more significant. So to reduce the exertion and enhance understanding, the experimental technique’s design is adapted, which considers all factors simultaneously and exhibits its outcome to the response variable.

This research study implements a two-level factorial design using the statistical tool Minitab 16. The two-level factorial design depicts that each

factor has two level values, i.e., High and Low. For the selected study, the Number of Cycles to failure or simply saying Cycles is the Response/Y variable, and all other affecting parameters/X variables are OBC, $P_{0.075}/P_{be}$ (Dust to Binder Ratio or simply saying DUST), Peak Force, VMA (Voids in Mineral Aggregate), Gmm @ Ini, Design Pbe, VFA. Etc. Initially, all the variables were included and used as input in Minitab 16 software. Results show that most factors come up to be insignificant. Hence to keep it simple, only significant variables are presented here, while insignificant variables are omitted after running the test for the first time (Model 1). The significant factors are presented in Table XIII, along with their abbreviation and high and low values. The table below presents the abbreviation for each factor considered for the study and its measurement units. Low-level and high-level values are also presented.

TABLE XIII
FACTORS AFFECTING THE TWO-LEVEL FACTORIAL DESIGN

| Factors | Abbreviations | Units | Low Level | High Level |
|--|---------------|-------|-----------|------------|
| Force/Peak Force | A | N | 2000 | 5000 |
| $P_{0.075}/P_{be}$ (Dust Proportion/Dust to Binder Ratio of the Gradation) | B | % | 1.15 | 1.23 |
| OBC (Optimum Bitumen Content) | C | % | 4.0 | 4.3 |

The approximations of the main effect and interaction effect are given in Table, obtained from running the factorial design in Minitab 16 software. These effects can be defined as “its mean difference in response of any factor at any particular, extreme values, i.e., low and high-level values”. In contrast, interaction effects can be defined as the “mean difference between

the effect of one factor at extreme values, i.e., high and low values of another factor”, or in other words, and it can be said that “it is a difference in the effect of one factor at a high level of other and affect one factor at a low level of another factor”.

TABLE XIV
EFFECT ESTIMATE FOR NO OF CYCLES TO FAILURE

| Main Factor | One Factor | | Two Factor | | | Three Factor | | |
|--------------------|------------|---------|--------------------------------|---------|---------|--------------------------------|---------|---------|
| | Effects | p value | Interaction | Effects | p Value | Interaction | Effects | p Value |
| Peak Force | -2049 | 0.00 | Peak Force* $P_{0.075}/P_{be}$ | -148 | 0.266 | Force* $P_{0.075}/P_{be}$ *OBC | 2993 | 0.00 |
| $P_{0.075}/P_{be}$ | -174 | 0.048 | Peak Force*OBC | 2225 | 0.00 | | | |
| OBC | 1305 | 0.00 | $P_{0.075}/P_{be}$ * OBC | -2030 | 0.00 | | | |

The Peak force, $P_{0.075}/P_{be}$ (Dust to Binder Ratio), and OBC effects estimates of 19 mm NMAS Gradations are presented in Table XIV. It shows that $P_{0.075}/P_{be}$ (Dust to Binder Ratio) has a higher value of p as compared to Peak Force and OBC, which means these factors slightly affect the re-

sponse variable (No of Cycles to Fatigue Failure/Cycles) while Peak Force and OBC has a more significant effect on the No of cycles to Fatigue Failure (Y/response variable). The negative signs, i.e., (+, -), show the nature of the relationship of effect. The negative signs show that it had indirect relation,

i.e., with a decrease in $P_{0.075}/P_{be}$ (Dust to Binder Ratio), the No of Cycles to Fatigue Failure/Cycles (Y/response variable) increases. Negative signs show that the inverse is true, which means that with an increase in Peak Force or the OBC, the No of Cycles to Fatigue Failure/Cycles (Y/response variable) decreases. The design of the experiment was conducted at a 95% confidence interval with a significant alpha $\alpha = 0.05$ for the said design. The significance of any factor can be judged by comparing the p -value to the significant level; if the p -value is less than 0.05, the factor is said to be significant.

TABLE XV
ANOVA FOR NO OF CYCLES TO FATIGUE FAILURE/ CYCLES (Y/RESPONSE VARIABLE)

| Sources | DF | Seq SS | Adj SS | Adj MS | F | p |
|---------------------|----|----------|----------|---------|--------|-------|
| Main Effects | 3 | 17635369 | 11042048 | 3680683 | 146.69 | 0.000 |
| 2 - Way Interaction | 3 | 3171489 | 4189312 | 1396437 | 55.65 | 0.000 |
| 3- Way Interaction | 1 | 1571051 | 1571051 | 1571051 | 62.61 | 0.000 |
| Residual Errors | 56 | 1405134 | 1405134 | 25092 | | |
| Lack of Fit | 24 | 262823 | 262823 | 10951 | 0.31 | 0.998 |
| Pure Errors | 32 | 1142311 | 1142311 | 35697 | | |
| Total | 63 | 23783043 | | | | |

The table represents the Analysis of Variance (ANOVA) of observed data for the No of Cycles to Fatigue Failure/Cycles (Y/response variable) of 19 mm NMAS mixes up to three-way interaction effects. It is stated in notified from the table above that degree of freedom for the main effect is three (03), which means there are three parameters explaining the variation of No of Cycles to Fatigue Failure/Cycles (Y/response variable), i.e., Peak Force, $P_{0.075}/P_{be}$ (Dust to Binder Ratio), and OBC. The significance of factors is refereed by comparing the p -value to $\alpha = 0.05$ and the value of F (normally greater than considered to be significant). Here the main effect along with 2-Way and 3-Way is observed as significant as the p -value is less than 0.05, and F is greater than 10.

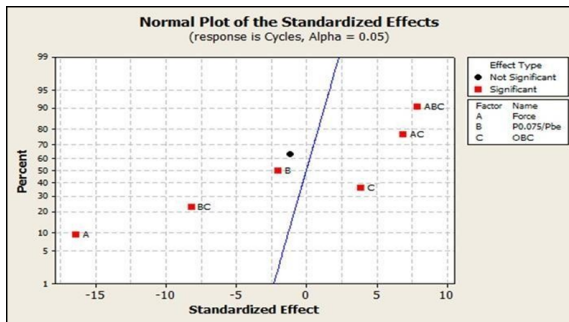


Fig. 6. Normal Plot for No of Cycles to Fatigue Failure/Cycles (Y/response Variable)

The figure indicates the factors selected for the study of 19 mm NMAS mixes that come out to be significant or otherwise. The black dots denote that factors are insignificant (one in this case, i.e., the interaction of peak force and dust-to-binder ratio), while the red squares show significant factors as represented in the legend. The Peak Force (Force) and OBC have a significant influence (indirect relation) on the No of Cycles to Fatigue Failure/Cycles (Y/response variable), and their strength can be judged by their distance away from the reference line. While $P_{0.075}/P_{be}$ (Dust to Binder Ratio) is also on the negative side, which means it also has a significant effect (indirect relation) on the No of Cycles to Fatigue Failure/Cycles (Y/response variable), but its strength is low, as can be judged by the distance

from the reference line. Two-way and three-way also significantly affect the No of Cycles to Fatigue Failure/Cycles (Y/response variable), which can be seen from the figure.

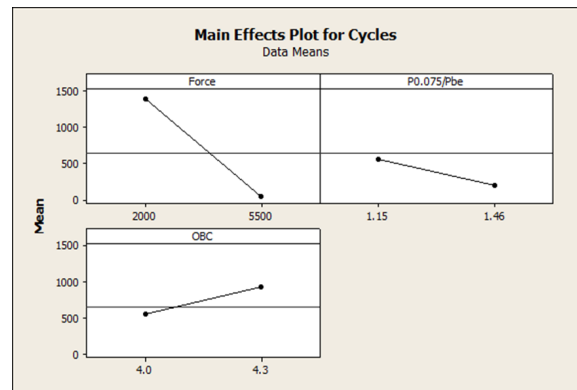


Fig. 7. Main Effect Plot for No of Cycles to Fatigue Failure/Cycles (Y/response variable)

The Figure illustrates the main effect plot for the 19 mm NMAS mixtures. This plot explains the main effect versus the low and high-level factors considered for this study, and the line's sharp slope illustrates a strong relationship between the response parameter and the response variable. Force (Peak Force) has a sharp slope which shows it is a significant variable and affects the No of Cycles to Fatigue Failure/Cycles (Y/response variable) inversely, as suggested by the slope of the line. In contrast, $P_{0.075}/P_{be}$ (Dust to Binder Ratio) is also a significant parameter explaining the No changes of Cycles to Fatigue Failure/Cycles (Y/response variable) as it is also represented by the sharp slope and line descends, which denotes that $P_{0.075}/P_{be}$ (Dust to Binder Ratio) is directly related to No of Cycles to Fatigue Failure/Cycles (Y/response variable). OBC has little significant effect impact on No of Cycles to Fatigue Failure/Cycles (Y/response variable).

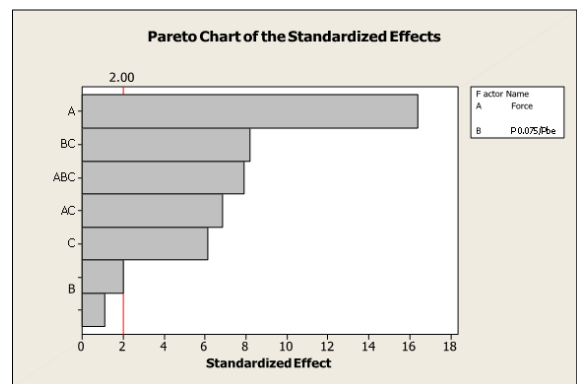


Fig. 8. Pareto Chart for No of Cycles to Fatigue Failure/Cycles (Y/response Variable)

The significance of the factor and interaction effects for 19 mm NMAS mixes is given in Figure, i.e., the Pareto chart. For 19 mm NMAS mixes, VFA is the most significant factor affecting the No of Cycles to Fatigue Failure/Cycles (Y/response variable). Meanwhile, Peak Force/Force and $P_{0.075}/P_{be}$ (Dust to Binder Ratio) are also significant parameters affecting the No of Cycles to Fatigue Failure/Cycles (Y/response variable) as their bars are passing the t -critical value for a 95% confidence interval.

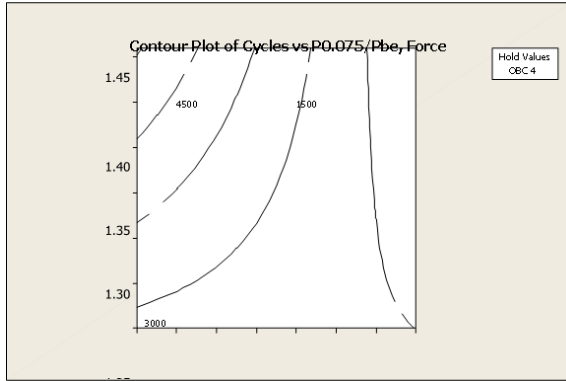


Fig. 9. Response Plot at Low Level of $P_{0.075}/P_{be}$ (Dust to Binder Ratio) & Peak Force

The Figure denotes the Contour response plot, which specifies a series of experiments on various 19 mm NMAS wearing course mixtures. The No of Cycles to Fatigue Failure/Cycles (Y/response variable) values increase in $P_{0.075}/P_{be}$ (Dust to Binder Ratio) and decrease with an increase in Peak Force/Force. The best way to understand the plot is to consider it like a topological map with these lines indicating the contours of an equal No of Cycles to Fatigue Failure/Cycles (Y/response variable). The curvature of the line shows the interaction between $P_{0.075}/P_{be}$ (Dust to Binder Ratio) and Peak Force/Force at a low level. Keeping the Peak Force/Force, the No of Cycles to Fatigue Failure/Cycles (Y/response variable) value can be predicted at any $P_{0.075}/P_{be}$ (Dust to Binder Ratio). It can be done by drawing a line parallel to the Peak Force/Force axis across the contour plot. Similarly, keeping the $P_{0.075}/P_{be}$ (Dust to Binder Ratio) constant, No of Cycles to Fatigue Failure/Cycles (Y/response variable) can be obtained at any point of Peak Force/Force by drawing a line parallel to the vertical axis.

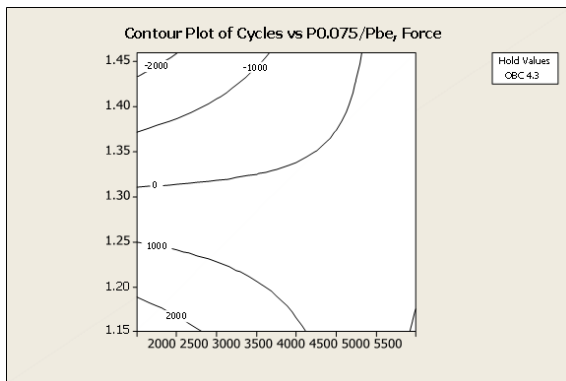


Fig. 10. Response Plot at High Level of $P_{0.075}/P_{be}$ (Dust to Binder Ratio) & Force/Peak Force

The Figure demonstrates the Contour response surface plot. It can be inferred in the same way as that of Figure 10, but with only modification, it integrated the high-level value of $P_{0.075}/P_{be}$ (Dust to Binder Ratio) and Peak Force/Force. Figure 11 represents three dimensional (3D) view of No of Cycles to Fatigue Failure/Cycles (Y/response variable) versus $P_{0.075}/P_{be}$ (Dust to Binder Ratio) and Peak Force/Force. It can be inferred

that No of Cycles to Fatigue Failure/Cycles (Y/response variable) increases with a decrease in Peak Force. While No of Cycles to Fatigue Failure/Cycles (Y/response variable) can be predicted for $P_{0.075}/P_{be}$ (Dust to Binder Ratio) and Peak Force/Force values other than stated in the test merely by drawing a line from required $P_{0.075}/P_{be}$ (Dust to Binder Ratio) and Peak Force/Force onto the No of Cycles to Fatigue Failure/Cycles (Y/response variable). This plot is a low-level surface plot and is useful for determining the intermediate & desirable values for the response variable.

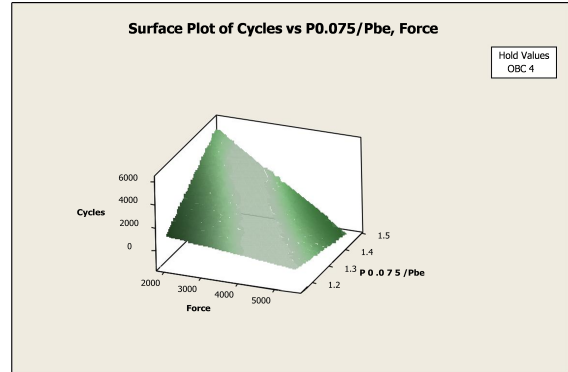


Fig. 11. Low-Level Surface Plot

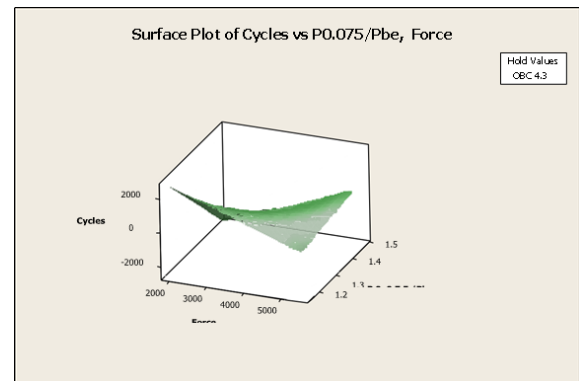


Fig. 12. High-Level Surface Plot

The Figure represents the low-level surface plot for No of Cycles to Fatigue Failure/Cycles (Y/response variable) at low $P_{0.075}/P_{be}$ (Dust to Binder Ratio) and Peak Force/Force.

D. Model Validation

Model validation is a method to compute the pertinence/approach/appropriateness to predict the observed data using the regression model. There are various approaches and techniques for model validation. However, for this research study, Mean Absolute Percentage Error (MAPE) is used, which can be defined as "the mathematical difference between observed and fitted data value divided by observed value and taking an average of that gives a mean absolute error, and if 100 is multiplied, it will yield a percentage error". It is given by the Equation 1.

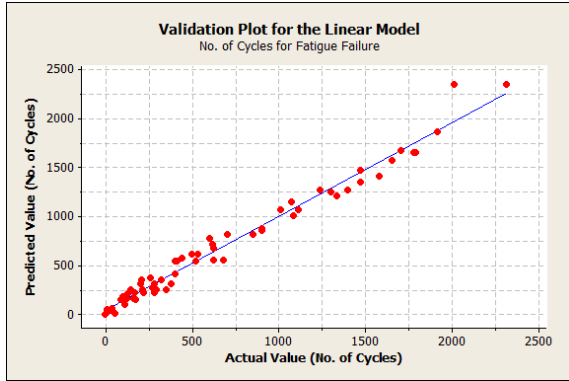


Fig. 13. Validation Plot for Model

At = Actual Value, Ft = Fitted Value, The MAPE of this model is 02%. The Figure shows the validation plot (MAPE) for the model. The more the data values are close to the 45° line better the model has the predictive capability. It is evident from the figure that most of the data values are close to the line, which shows that the model is very good and defines its good predictive ability.

E. Sensitivity Analysis

Sensitivity analysis describes the influence of various independent variables (Input) on the dependent variable (Output) under certain predefined conditions. This analysis is done within a boundary condition defining the input variable. Based on this input or independent variables, sensitivity analysis proposes the extent to which each output is sensitive to particular input variables or variations in the input factors. It can be suitable while testing the models' robustness or output based on certain input parameters.

The model representation and plots indicate that the No of Cycles to Fatigue Failure/Cycles (Y/response variable) values increase in $P_{0.075}/P_{be}$ (Dust to Binder Ratio) and decrease with an increase in Peak Force/Force. Sensitivity Analysis also shows the interaction between $P_{0.075}/P_{be}$ (Dust to Binder Ratio) and Peak Force/Force at different levels. Keeping the Peak Force/Force, the No of Cycles to Fatigue Failure/Cycles (Y/response variable) value can be predicted at any $P_{0.075}/P_{be}$ (Dust to Binder Ratio). Similarly, keeping the $P_{0.075}/P_{be}$ (Dust to Binder Ratio) constant, No of Cycles to Fatigue Failure/Cycles (Y/response variable) can be obtained at any point of Peak Force/Force.

F. Indirect Tensile Strength Test

The stress-strain template was opened, and the stress-strain test was conducted by applying a compressive load of 50 mm/min at 25°C.



Fig. 14. Failed Specimen



Fig. 15. Before and After Test for IDT

The table shows the IDT test results recorded by UTM-25 for each Gradation (ARZ, TRZ, and BRZ)

TABLE XVI
PEAK FORCE VALUE IN IDT TEST

| Gradation | % Bitumen | Diameter (inch) | Peak Force (KN) |
|-----------|-----------|-----------------|-----------------|
| ARZ | 4.3 | 4 | 6147 |
| BRZ | 4.2 | 4 | 7659 |
| TRZ | 4.0 | 4 | 8335 |
| NHA A | 4.1 | 4 | 7142 |

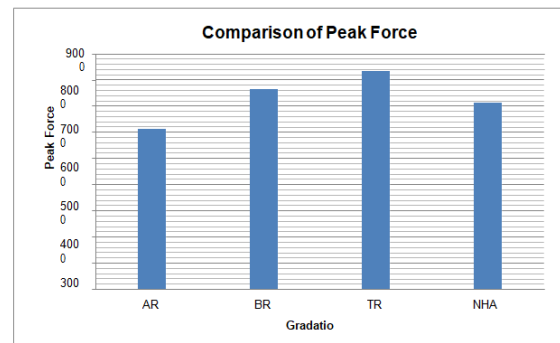


Fig. 16. Indirect Tension Test Peak Values for Different Gradations

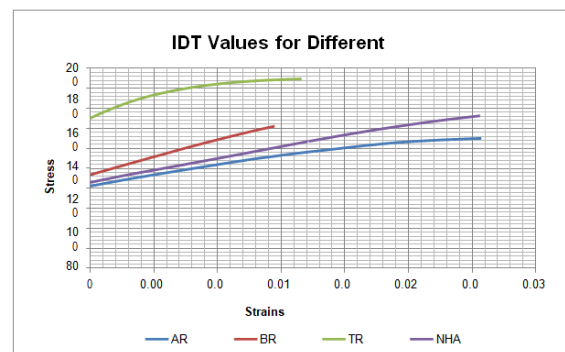


Fig. 17. IDT Values for Different Gradations (Stress versus Strain)

The results show reasonable variability for all mixes with less than 30 percent COV values. The results indicate that the TRZ mix is the most resistant to fracture of the tested mixes based on the bending strain value achieved at maximum load. This is indicative that the mix is the most ductile and has the most potential to elongate before tensile crack failure. Therefore, this mix would have all tested mixes' best laboratory fracture resistance properties. While an increase in asphalt content would be expected to cause an increase in the strain at maximum load. This might be

why the TRZ is observed to be the best among the mixes. One thing is evident from the results NHA A and ARZ both produce more strain at the given set of loads. They can take more strain. This might be the reason for their better performance in the Repeated TFT test because it provides load in haversine form. Detailed statistical data can be found in Appendix B.

G. Moisture Susceptibility Test

AASHTO T283 is the test procedure that helps us to describe the resistance of bituminous mixes against stripping. This is evaluated by the Indirect Tensile Strength (ITS). The results obtained for the ITS for dry and wet samples are presented. Three (03) replicate samples were tested for each Gradation, and the averaged value was taken individually. The Average strength in dry and wet conditions is presented in Table XVII. TSR was calculated too. Average Strength in both Wet and dry conditions was obtained using the UTM-25 and Average Tensile Strength Ratio for three samples of different gradations.

TABLE XVII
COMPARISON OF STRENGTHS AND TSR CALCULATION

| Gradation | Wet Strength | Dry Strength | TSR |
|-----------|--------------|--------------|-------|
| ARZ | 5747 | 6137 | 0.936 |
| BRZ | 6373 | 7690 | 0.827 |
| TRZ | 7383 | 8380 | 0.881 |
| NHA A | 6262 | 7151 | 0.876 |

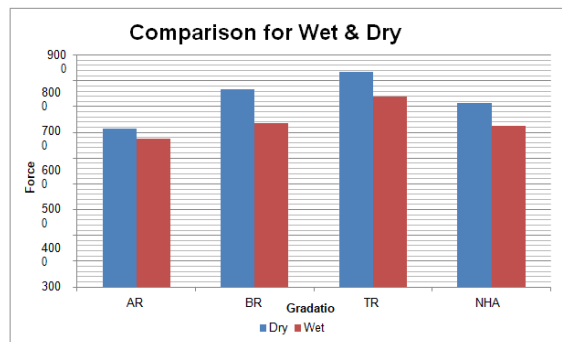


Fig. 18. Comparison of Strengths for Wet & Dry Samples

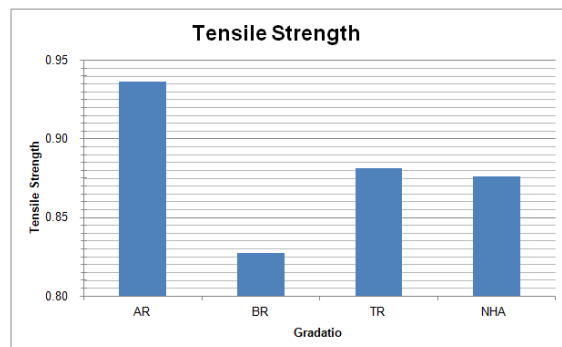


Fig. 19. Tensile Strength Ratio Comparison

IV. CONCLUSION AND RECOMMENDATIONS

The research aimed to review the Permanent Deformation and Fracture effect of Superpave three (03) gradations that passed from Above, Through, and Below the Restricted Zone in contrast to the NHA "Class A" Gradation

that is already in use in industry in Pakistan. Three (03) different testing types were conducted using the same Testing Machine, i.e., UTM - 25. These tests were IDT, Repeated Indirect Tensile Fatigue Test (ITFT), and Moisture Susceptibility Test (using TSR). These tests were performed to evaluate the performance of four (04) gradations in total, i.e., ARZ, BRZ, TRZ, and NHA Class A. Aggregates were procured from native quarry site, i.e., Margalla, whilst 60/70 ARL grade bitumen was procured from Attock Oil Refinery. Samples were prepared at 165°C and compacted at 135°C, and the volumetric of each Gradation was carried out separately according to Superpave Manual (SP-2, 2001). After calculating OBC and volumetric, performance testing was carried out in a Universal Testing Machine (UTM-25). Later statistical analysis was done on the data/results obtained. Two Level Factorial design was formulated. At first, eight (08) factors were selected and checked for significance. Out of eight (08) factors, only three (03) were coming to be significant. Those were selected for the model building with No of Cycles to Fatigue Failure as a Y/response variable (results obtained from the ITFT test). The three significant (03) factors were Peak Force/Force, $P_{0.075}/P_{be}$ (Dust to Binder Ratio), and OBC OBC versus the Y/response variable (No of Cycles to Fatigue Failure). Similarly, IDT was performed along with Moisture Susceptibility by calculating the Tensile Strength Ratio of samples. The results of all these tests are presented in this chapter and are explained in detail.

Following are the recommendation points.

1. Evaluate the effect of the same Gradation with different aggregate sources and binder grades and then evaluate the Gradation or the binder grade that performs better for the same performance tests.
2. To investigate the effect of water on stripping/moisture susceptibility same gradation with the same aggregate source and lime-modified binder should be used, and then evaluate the Gradation that performs better. (Lime reduces stripping, so better variability can be seen by modifying the binder with lime and checking for the best Gradation).
3. Compare the same NMAS with different mix design method like the Marshall Design method and then find the volumetric and performance of the mixtures that performs better.

References

- [1] E. Mogaji, I. A. Adekunle, and N. P. Nguyen, "Enhancing transportation service experience in developing countries: A post pandemic perspective," in *The Future of Service Post-COVID-19 Pandemic*. Singapore: Springer, 2021.
- [2] M. S. Anjum, S. M. Ali, M. A. Subhani, M. N. Anwar, A.-S. Nizami, U. Ashraf, and M. F. Khokhar, "An emerged challenge of air pollution and ever-increasing particulate matter in Pakistan; a critical review," *Journal of Hazardous Materials*, vol. 402, pp. 1-15, 2021. doi: <https://doi.org/10.1016/j.jhazmat.2020.123943>
- [3] M. Previtali, R. Brumana, and F. Banfi, "Existing infrastructure cost effective informative modelling with multisource sensed data: Tls, mms and photogrammetry," *Applied Geomatics*, vol. 14, pp. 1-20, 2020. doi: <https://doi.org/10.1007/s12518-020-00326-3>
- [4] H. Zhang and C. Sun, "Cost-effective iron-based aqueous redox flow batteries for large-scale energy storage application: A review," *Journal of Power Sources*, vol. 493, pp. 1-20, 2021. doi: <https://doi.org/10.1016/j.jpowsour.2020.229445>
- [5] C. Bulei, M. Todor, T. Heput, and I. Kiss, "Directions for material recovery of used tires and their use in the production of new products intended for the industry of civil construction and pavements," in *IOP Conference Series: Materials Science and Engineering*, Hunedoara, Romania. IOP Publishing, 2018. doi: <https://doi.org/10.1088/1757-899X/294/1/012064>

- [6] T. Islam, "Rheology and surface free energy of modified asphalt binder containing anti-stripping additives," Ph.D. dissertation, Memorial University of Newfoundland, Newfoundland, Canada, 2022.
- [7] N. A. Memon, N. I. M. Yusoff, S. F. Jafri, and K. Sheeraz, "Rheological findings on storage stability for chemically dispersed crumb rubber modified bitumen," *Construction and Building Materials*, vol. 305, p. 124768, 2021. doi: <https://doi.org/10.1016/j.conbuildmat.2021.124768>
- [8] B. Khamon, "Study of factors affecting strength of sealing in the product packing process by utilizing central composite design," *International Journal of Technology and Engineering Studies*, vol. 4, no. 2, pp. 77-85, 2018. doi: <https://dx.doi.org/10.20469/ijtes.4.10001-3>
- [9] F. Canestrari and L. P. Ingrassia, "A review of top-down cracking in asphalt pavements: Causes, models, experimental tools and future challenges," *Journal of Traffic and Transportation Engineering*, vol. 7, no. 5, pp. 541-572, 2020. doi: <https://doi.org/10.1016/j.jtte.2020.08.002>
- [10] L. F. Walubita, L. Fuentes, S. I. Lee, O. Guerrero, E. Mahmoud, B. Naik, and G. S. Simate, "Correlations and preliminary validation of the laboratory monotonic Overlay Test (OT) data to reflective cracking performance of in-service field highway sections," *Construction and Building Materials*, vol. 267, p. 121029, 2021. doi: <https://doi.org/10.1016/j.conbuildmat.2020.121029>
- [11] P. Tavassoti, M. Solaimanian, and X. Chen, "Characterization of fatigue performance of cold mix recycled asphalt mixtures through uniaxial tension-compression testing," *Construction and Building Materials*, vol. 329, p. 127155, 2022. doi: <https://doi.org/10.1016/j.conbuildmat.2022.127155>
- [12] F. Tahmoorian and B. Samali, "Laboratory investigations on the utilization of RCA in asphalt mixtures," *International Journal of Pavement Research and Technology*, vol. 11, no. 6, pp. 627-638, 2018. doi: <https://doi.org/10.1016/j.ijprt.2018.05.002>
- [13] O. C. Assogba, Y. Tan, Z. Sun, N. Lushinga, and Z. Bin, "Effect of vehicle speed and overload on dynamic response of semi-rigid base asphalt pavement," *Road Materials and Pavement Design*, vol. 22, no. 3, pp. 572-602, 2021. doi: <https://doi.org/10.1080/14680629.2019.1614970>
- [14] O. C. Assogba, Y. Tan, X. Zhou, C. Zhang, and J. N. Anato, "Numerical investigation of the mechanical response of semi-rigid base asphalt pavement under traffic load and nonlinear temperature gradient effect," *Construction and Building Materials*, vol. 235, p. 117406, 2020. doi: <https://doi.org/10.1016/j.conbuildmat.2019.117406>
- [15] I. M. ud Din, M. S. Mir, and M. A. Farooq, "Effect of freeze-thaw cycles on the properties of asphalt pavements in cold regions: A review," *Transportation Research Procedia*, vol. 48, pp. 3634-3641, 2020. doi: <https://doi.org/10.1016/j.trpro.2020.08.087>
- [16] Z. Fatkhurrohman, "Effect of fiber volume fraction to tensile strength in composites polyester reinforced Sugar Palm Fiber (SPF)," *Journal of Advances in Technology and Engineering Studies*, vol. 4, no. 6, pp. 222-229, 2018. doi: <https://doi.org/10.20474/jater-4.6.2>
- [17] M. Y. Fattah, M. M. Hilal, and H. B. Flyeh, "Evaluation of the mechanical stability of asphalt mixture using the gyratory compactor," *International Journal of Pavement Research and Technology*, vol. 12, pp. 508-518, 2019. doi: <https://doi.org/10.1007/s42947-019-0061-9>
- [18] M. R. Pouranian and J. E. Haddock, "A new framework for understanding aggregate structure in asphalt mixtures," *International Journal of Pavement Engineering*, vol. 22, no. 9, pp. 1090-1106, 2021. doi: <https://doi.org/10.1080/10298436.2019.1660340>
- [19] Y. Zhang, X. Luo, I. Onifade, X. Huang, R. L. Lytton, and B. Birgisson, "Mechanical evaluation of aggregate gradation to characterize load carrying capacity and rutting resistance of asphalt mixtures," *Construction and Building Materials*, vol. 205, pp. 499-510, 2019. doi: <https://doi.org/10.1016/j.conbuildmat.2019.01.218>
- [20] H. Ozer, I. L. Al-Qadi, J. Lambros, A. El-Khatib, P. Singhvi, and B. Doll, "Development of the fracture-based flexibility index for asphalt concrete cracking potential using modified semi-circle bending test parameters," *Construction and Building Materials*, vol. 115, pp. 390-401, 2016. doi: <https://doi.org/10.1016/j.conbuildmat.2016.03.144>
- [21] M. Y. Fattah, M. M. Hilal, and H. B. Flyeh, "Assessment of mechanical stability performance of asphalt mixture using superpave gyratory compactor," *Journal of Transportation Engineering, Part B: Pavements*, vol. 145, no. 2, pp. 1-13, 2019. doi: <https://doi.org/10.1061/JPEODX.0000102>